Nanoscale

Accepted Manuscript

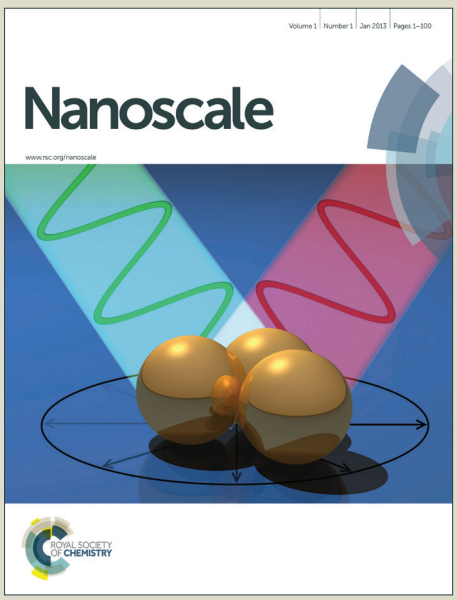

ROYAL SOCIETY OF CHEMISTRY

www.rsc.org/nanoscale

Cite this: DOI: 10.1039/c0xx00000x

www.rsc.org/xxxxxx

ARTICLE

Highly Sensitive Monitoring of Catalytic Reactions in Situ by Surface Enhancement Raman Spectroscopy on Multifunctional Fe_3O_4/C/Au NPs

Wenya Cai,[a] Xianghu Tang,[a,b] Bai Sun[a]* and Liangbao Yang[a]*

Received (in XXX, XXX) Xth XXXXXXXXX 20XX, Accepted Xth XXXXXXXXX 20XX

DOI: 10.1039/b000000x

In this paper, multifunctional Fe_3O_4/C/Au nanoparticles (NPs) which integrated catalytically active small Au NPs with surface-enhanced Raman scattering (SERS) active large Au NPs, were fabricated via a facile method and be employed for in situ SERS monitoring of a catalytic reaction *p*-nitrothiophenol (*p*-NTP) to *p*-aminothiophenol (*p*-ATP). Besides the effect of magnet power was tested and it was demonstrated that SERS intensity of the reaction system was stronger and reaction proceeded more smoothly since that more hot spots existed and also could remain the same in the magnetic field, due to which, catalytic rate could be determined.

Introduction

Catalytic activity and the reaction kinetics has been investigated frequently using UV/Vis absorption[1-4], which was simple, stable and repeatable and thus it is one of the most common method used on catalytic research. However, it exhibits relatively low sensitivity and provides very limited chemical information, which is a disadvantage in tracking the reaction process comparing with surface-enhanced Raman scattering (SERS) which combines the advantages of high chemical specificity (vibrational Raman scattering), high sensitivity (electromagnetic and chemical enhancement), and surface selectivity (near-field enhancement)[5-7]. On the other hand, in principle, reactions at the surface of metal structures should be studied using molecular surface specific spectroscopic techniques, the most versatile of these is SERS[8]. Due to that, these years, the application of SERS on in situ monitoring catalytic reactions has been made a great progress, e.g., Wei Xie et al. demonstrated the in situ SERS monitoring of platinum-catalyzed reaction via rationally designed bifunctional, raspberry-like Au/Pt/Au core/shell particles[9]. Virginia Joseph et al. immobilized the separate gold and platinum nanoparticles simultaneously on a glass surface to monitor a catalytic reaction by SERS[8]. Sebastian Schlücker et. al. presented label-free in situ SERS monitoring using rationally designed plasmonic superstructures[5]. Despite of the progress achieved during the latest years, the application of in situ SERS on monitoring catalytic reactions also has its limitations: (1) since neither the small nor the large Au NPs alone exhibit both desired properties: catalytic and SERS activity, catalysts and substrates were acted by different material and commonly the catalysts such as platinum and palladium may diminish the SERS enhancement[7, 10, 11]; (2) nanocomposites should be immobilized to eliminate the influence of moving of substrates[8], which is complicated and difficult to use chemical immobilizing method;

Magnetic composite nanomaterials consisting of more than two functional properties have been attracting much research interests due to the exhibiting of multifunction in a single entity. In particular, integration of ferromagnetic oxides and noble metal nanoparticles(NPs) in composites results in simultaneous magnetic activity and optical response where the optical property of the whole system could be modulated by application of an external magnetic field, for instance, Shaojun Guo et.al. prepared Fe_3O_4/Metal using APTMS as a linker, which construct hybrid nanostructures that display near-IR absorption, high catalytic activity[12]. Zhiyong Bao fabricated Ag NPs-coated Fe_3O_4 microspheres as a novel surfactant-free SERS substrate through a solid-phase thermal decomposition reaction and the SERS sensitivity of the fabricated nanocomposites could be increased by magnetic-field-directed self-assembly of the composite substrates[13]. It can be found from these results that noble metal loaded Fe_3O_4 nanocomposites can be used as SERS substrates and catalysts with high sensitivity.

Here we demonstrate a facile approach for integrating catalytically active small Au NPs with SERS-active large Au NPs into a single bifunctional Fe_3O_4/C/Au core/shell nanostructures. We employed these designed plasmonic superstructures to monitor a catalytic reaction p-nitrothiophenol (*p*-NTP) to p-aminothiophenol (*p*-ATP) with sodium borohydride by in situ SERS and determining the reaction kinetics and rate constant in the presence and absence of magnetic field. It is demonstrated that (1) this core/shell nanoparticle has a high SERS enhancement and also catalytic activity; (2) magnetic field can make the Fe_3O_4/C/Au NPs immobilized on silicon wafer and hot spots remains the same so that catalytic reaction can proceed smoothly and rate constant can be determined. This material can overcome the limitations mentioned above and provided a possibility to be further applied for SERS in situ monitoring.

Experimental

Apparatus

Field emission scanning electron microscope (FESEM) images were taken with a FESEM (Quanta 200 FEG) operated at an accelerating voltage of 10.0 kV. Transmission electron microscopy (TEM) images were recorded by a JEOL 2010 high resolution transmission electron microscope, equipped with X-ray energy dispersive spectroscopy (EDS) and selected area electron diffraction (SAED) system. Raman spectra were carried out on a LabRAM HR800 confocal microscope Raman system (Horiba Jobin Yvon) using a He-Ne laser operating at 632.8 nm. The laser beam was focused on the sample in a size of about 1μm using a 50×microscope objective. To follow the reaction, spectra with 1 s aquisition time were acquired every 2 s.

Reagents and materials

Iron(Ⅲ) chloride hexahydrate($FeCl_3·6H_2O$), ethylene glycol(EG), sodium acetate anhydrous(NaAc), polyethylene glycol(PEG), Sodium borohydride($NaBH_4$), tetrachloroauric acid tetrahydrate ($HAuCl_4·4H_2O$), trisodium citrate dehydrate ($C_6H_5Na_3O_7.2H_2O$) and 3-aminopropyltrimethoxysilane (APTMS) were purchased from Shanghai Chemical Reagent Company (Shanghai, China). p-nitrothiophenol (*p*-NTP), p-aminothiophenol (*p*-ATP) and 2-naphthalenethiol (2-NT) were purchased from aladdin company. The reagents were all of analytical grade and used without further purification. Ultrapure water (>18.0 MΩ·cm) was purified using a Millipore Milli-Q gradient system throughout the experiment.

Synthesis of Au NPs

Au NPs were synthesized by reduction of $HAuCl_4$ using trisodium citrate[14]. Typically, freshly prepared aqueous trisodium citrate solution (2 mL, 1 wt%) was quickly added to a boiling aqueous solution of $HAuCl_4$ (100 mL, 0.25 mM) under vigorous stirring and refluxing. After several minutes, the color of the solution changed from blue to brilliant red. After boiling for 40 min, the heat source was removed to allow the reaction solution to cool to room temperature. Au NPs about 25 nm were obtained.

Synthesis of Fe_3O_4 NPs

The synthesis was carried out according to the literature[15] with a small modification. A typical experiment was as follows: first, $FeCl_3·6H_2O$ (1.35 g) was dissolved in ethylene glycol (40 mL) to form a clear solution. Polyethylene glycol 10000 (1.0 g) and $NaAc·3H_2O$ (3.6 g) were added. The mixture was stirred until the reactants were fully dissolved and then heated at 200 °C for 12 h. The products were separated with magnet, rinsed with deionized water and ethanol, and dried under vacuum at 60 °C for 6 h.

Fabrication of Au NPs coated Fe_3O_4/C NPs

A typical procedure was as follows. First, 0.5 g Fe_3O_4 NPs and glucose were mixed and then heated at 180 °C for 12 h and Fe_3O_4/C NPs were obtained. Next, 50 mg Fe_3O_4/C NPs were functionalized with APTMS under mechanical stirring for 4 h, and then, as-synthesized Au NPs solution was added to the above treated Fe_3O_4/C NPs with ultrasonication. This process was repeated until the color of Au sol was not changed. The products were collected by magnet followed by washed with water.

Characterization of catalytic properties of Fe_3O_4/C/Au NPs

The procedure of Characterization of catalytic properties for Fe_3O_4/C/Au was as follows. (1) Functionalization of the surfaces of nanocoposite. Functionalization with *p*-NTP and 2-NT was performed by immersion of the Fe_3O_4/C/Au NPs(0.5 mg) in a mixture of 10^{-4} M *p*-NTP and 10^{-4} M 2-NT for 2 hour. (2) Materials obtained in (1) were added to the silicon wafer in magnetic field outside. (3) The catalytic reduction was started by dropping a mixture of 10^{-2} M sodium borohydride. To follow the reaction, spectra with 1 s aquisition time were acquired every 2 s.

Results and Discussion

Scheme 1 shows the synthesis of multifunctional Fe_3O_4/C/Au. Firstly, Fe_3O_4 NPs were synthesized according to literature[14] and then incubated with glucose to form a thin inert carbon shell coating around the Fe_3O_4 core. Next, the obtained carbon-encapsulated Fe_3O_4 NPs are then incubated again with APTMS to functionalize their surface with amino groups. Au NPs synthesized referring to literature[15] subsequently mixed with the amino-functionalized Fe_3O_4 NPs and captured by the amino groups[12].

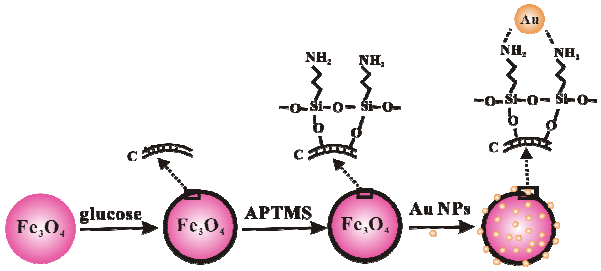

Scheme **1**. Synthesis of Fe_3O_4/C/Au nanostructures.

The surface morphology of the obtained Fe_3O_4/C and Fe_3O_4/C/Au were observed by SEM and TEM (Fig.1). The diameter of the magnetic Fe_3O_4 NP obtained was about 350 nm and the thickness of linker C layer was uniform, about 12 nm (Fig.1A and Fig.1B). After functionalized with NH_2 groups provided by APTMS, high-density of Au NPs have been immobilized on the surface of Fe_3O_4/C (Fig.1C and Fig.1D). Besides, seen from the size distribution of Au NPs (Fig.2B), it reveals that about 80% was 20-25 nm, but a few ones distributed less than 10 nm. The specific measurements of Au NPs sizes are come from the results of higher-magnification TEM images (the details are not shown). Generally, Au NPs with a diameter of less than 10 nm exhibit catalytic activity, but they cannot be used for efficient generation of SERS due to their very small scattering cross sections[5, 16, 17]; typically only Au NPs larger than 20 nm have sufficient plasmonic activity and provide the required SERS enhancement[5, 18]. Thus, Fe_3O_4/C/Au NPs displaying magnetization could be served as SERS substrates and catalysts.

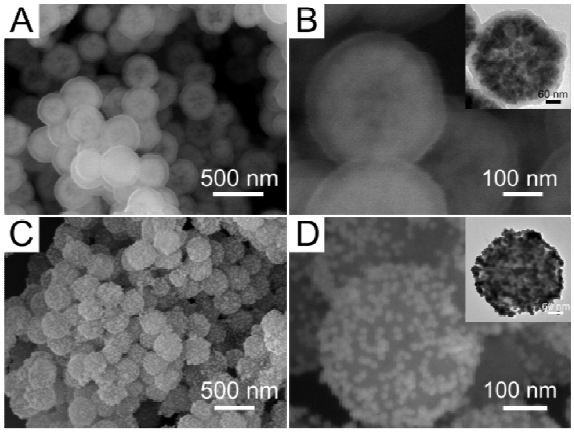

Fig.**1**. Typical SEM images of A, B) Fe_3O_4/C NPs; C, D) Fe_3O_4/C/Au NPs, the insets are the TEM images.

In order to figure out the atomic composition and elemental distribution, Fe_3O_4/C/Au NPs were analyzed by electron mapping image analysis (Fig.2). The elemental Fe, O, Au mapping images were acquired by visualizing the in elastically scattered electrons in the energy loss windows. The different color areas shown in parts C-F of Fig.2 indicate Fe-, O-, Au-enriched areas of Fe_3O_4/C/Au NPs, respectively. Among those, many tentacles in the outside of O-enriched areas and which is different from that of Fe maybe because that many active groups on the surface of Fe_3O_4 NPs. In conclusion, high-density of Au NPs have been immobilized on the surface of Fe_3O_4/C and core/shell superstructures formed.

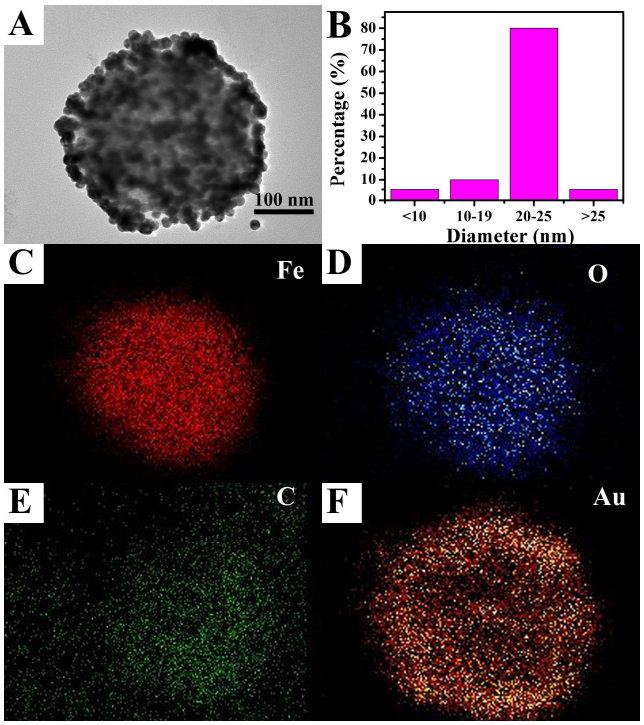

Fig.**2** (A) TEM image of the Fe_3O_4/C/Au NP. (B) Size distribution of Au NPs on the surface of Fe_3O_4/C. The elemental mapping of the Fe_3O_4/C/Au nanocomposites materials based on (C) Fe, (D) O, (E) C and (F) Au.

It is well documented that the reaction *p*-NTP to *p*-ATP can be catalyzed by noble metal nanoparticles with appropriate sizes, and the color changes involved in the reduction also provide a simple way based on spectroscopic measurements for monitoring the reaction kinetics[19, 20]. Thus, Fe_3O_4/C/Au NPs can also have catalytic activity in principle due to some Au NPs with the diameters less than 10 nm. Here we choose a molecular spectroscopy technology SERS to monitor the process of catalytic reaction, however, SERS intensity of reaction systerm was not stable during the reaction due to the inherent property of SERS.In order to eliminate the influence of substrates moving and solvent evaporation on SERS intensity, 2-NT was introduced as an intermediate under the magnetic field. Scheme 2 displays the representation of SERS monitoring using 2-NT as intermediate and Fe_3O_4/C/Au NPs as catalysis and substrates.

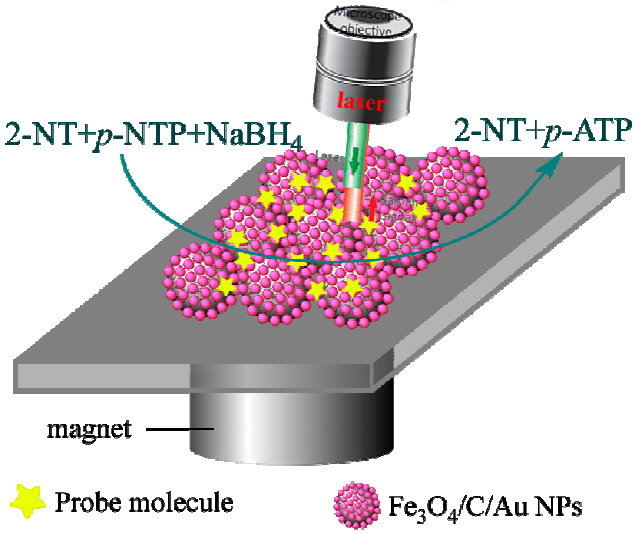

Scheme **2**. Representation of the reduction of *p*-NTP by sodium borohydride to give *p*-ATP.

In the presence and absence of magnetic field, SERS spectra of Fe_3O_4/C/Au NPs functionalized with a mixture of *p*-NTP and 2-NT at different time intervals after the addition of sodium borohydride were displayed in Fig.3A and Fig.3B, respectively. It is clearly reveal that before addition of sodium borohydride, characteristic bands of *p*-NTP and 2-NT were exhibited. After the addition of $NaBH_4$, with the reaction going on, new bands of 390 cm^{-1}, 1590 cm^{-1} appear and increases gradually, which can be assigned to corresponding aniline derivate R-NH_2[9]. Characteristic bands of *p*-NTP in 332cm^{-1}, 1572 cm^{-1} assigned to ring deformation and C=C stretching vibration respectively, decreases significantly[21], indicating the formation of *p*-ATP. Four minutes later, reaction started to level off.

As well known, determining the catalytic activity and the reaction kinetics are very important when new catalysts are developed, characterized, and introduced, which need to be accurate quantitative. Here the intensity of band at 724 cm^{-1} assigned to C-S stretching vibration[8, 21] of *p*-NTP, relative to the intensity of band at 599 cm^{-1} assigned to the ring deformation of 2-NT[22] was used for quantification. It is necessary to determine the reaction series before figuring out catalytic rate. The concentration of sodium borohydride is much higher than that of 2-NT and remains basically constant during the reaction. Therefore, pseudo-first-order kinetics with respect to *p*-NTP can be applied to evaluate the catalytic activity. The pseudo-first-order reaction rate constant k_1 can be determined by equation (1).

$$k_1=\ln(c_0/c_t) \quad (1)$$

Here, c_0 and c_t are concentration of reactant at the beginning and t moment respectively.

The relationship between SERS intensity and probe concentration can be determined by equation (2).

$$I_{SERS}=k.c \quad (2)$$

Here, c is concentration of probe molecular and k is constant for a substance. Thus, equation (3) can be obtained from equation (1) and (2).

$$k_1=\ln([p\text{-NTP}]_0/[p\text{-NTP}]_t)=\ln[(I_{724}/I_{599})_0/(I_{724}/I_{599})_t] \quad (3)$$

Here [*p*-NTP] is the concentration of *p*-NTP, and I_{724} and I_{599} are the intensities of the bands at 724 cm^{-1} and 599 cm^{-1},

respectively. The enlarged peaks at area 550-750 cm^{-1} of fig. 3A and fig. 3B were shown in supporting information. The logarithm of the ratio of the relative intensities at the beginning and at different time point t under the magnetic field is plotted in Fig.3C, which is a straight line fitting better than that in the absence of magnetic (Fig.3D) and its slope also the catalytic reaction rate constant is 0.0047 s^{-1} before the reaction level off, corresponding to the black data points.

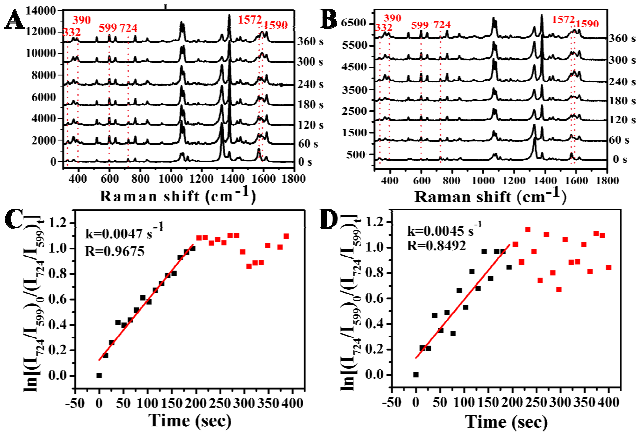

Fig.**3** SERS spectra recorded at selected time intervals after the addition of sodium borohydride to a *p*-NTP/2-NT-functionalized Fe_3O_4/C/Au NPs surface (A) in magetic field; (B) no magnetic field was used. Plots of $\ln[(I_{724}/I_{599})_0/(I_{724}/I_{599})_t]$ versus time for the reduction of *p*-NTP with Fe_3O_4/C/Au NPs as catalysts and substrates (C) in the magnetic field; (D) no magnetic field was used.

The reason for the different results obtained in the presence and absence of magnetic field was studied with the method that observing the changes of hot spots distribution after addition of $NaBH_4$, as is shown in Fig.4. Fig. 4A shows the optical image of Fe_3O_4/C/Au NPs by optical microscope platform of the Raman spectrometer in the presence magnetic field. It is clearly revealed that NPs spread more evenly than that in the absence of magnetic field (Fig.4B), since nanocomposites can not move and accumulate with the evaporation of solvent. Fig.4C and Fig.4E show area scanning mapping of the SERS spectra corresponding to dotted square area in Fig.4A, meanwhile Fig.4D and Fig.4F are obtained corresponding to dotted square area in Fig.4B, based on the intensity of the spectral band at 1345 cm^{-1} of *p*-NTP and 1079 cm^{-1} of *p*-ATP, the product of in situ reduction. It is interesting and important to find that the profile of Fig.4E is similar to Fig.4C while Fig.4F and Fig.4D are completely different, which indicates that the presence of magnetic field can immobilized the substrates so that hot spots remains the same and catalytic reaction can proceed smoothly and rate constant can be determined.

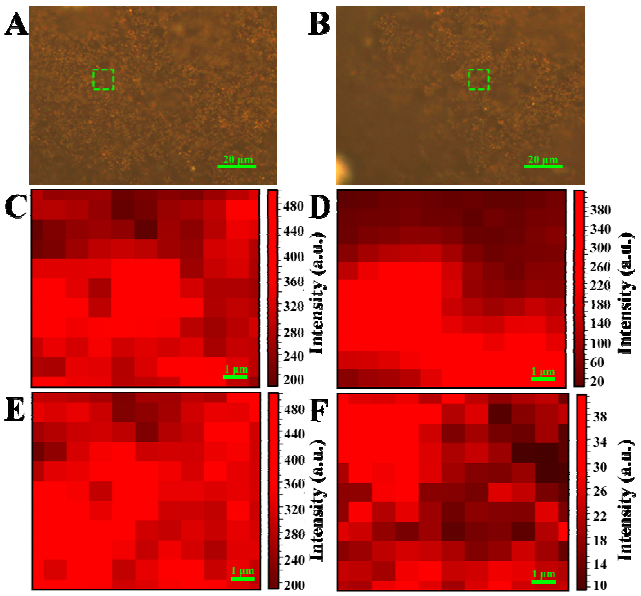

Fig.**4** The optical image of Fe_3O_4/C/Au NPs spread on the surface of silicon wafer (A) in the presence and (B) in the absence of magnetic field; area scanning mapping based on the intensity of the spectral band at (C,D) 1345 cm^{-1} of *p*-NTP; (E,F) 1079 cm^{-1} of *p*-ATP.

At the same time, we can find that the intensity of *p*-NTP and *p*-ATP in the absence of magnetic field was lower than that obtained in the magnetic field. For testing the magnet power of the experiments, two different experiments are devised. First, aliquots of the nanocomposites with 10^{-5} M *p*-NTP are cast into a silicon wafer. In the second experiment, the nanocomposites particles are collected with a magnet. As shown in Fig.5, we can find that the assembled nanoparticles using the magnet show apparently stronger SERS signals (curve a). Many studies have demonstrated that the assembled nanoparticles exhibit a high surface enhancement factor due to precise control over the gap between them[23, 24]. So there is an impotent role of the magnet in this experiment.

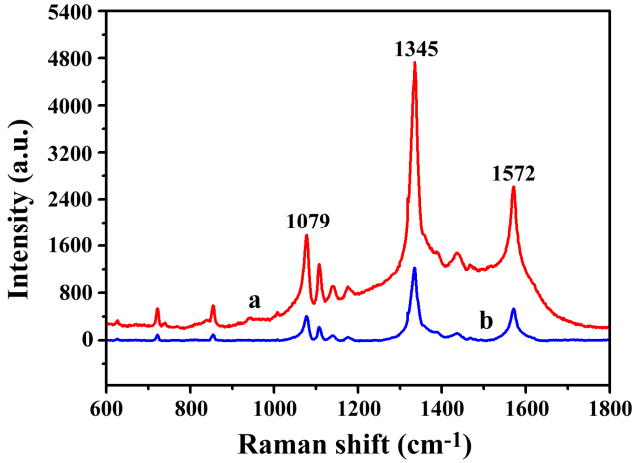

Fig.**5** SERS spectra of 10^{-5} M *p*-NTP adsorbed on substrate: a: collected using the magnet, b: without using the magnet.

Conclusion

In summary, we have rationally designed and synthesized core/shell structures Fe_3O_4/C/Au comprising different sizes of Au

NPs. The composites obtained were employed for in situ SERS monitoring of the reaction *p*-NTP to *p*-ATP and determining catalytic rate in the presence and absence of magnetic field. It was found that the intensity of probe molecules was stronger and reaction proceeded more smoothly in the magnetic field since that Fe_3O_4/C/Au NPs cannot move and spread more evenly and intensively, so that hot spots can remain unchanged after reaction and catalytic rate can be determined. This work can provide a way for characterizing the species and determining the rate constants in the similar experiment.

Acknowledgements

This work was supported by the National Science Foundation of China (No. 20871089, 21271136, 61104205, 51002157, 21177131), the Important Project of Anhui Provincial Education Department (KJ2010ZD09) and the program of Innovative Research Team of Suzhou University (2013kytd02).

[a] Institute of Intelligent Machines, Chinese Academy of Sciences, Hefei 230031, China. Fax: (+86)551-65592420; E-mail: lbyang@iim.ac.cn, bsun@iim.ac.cn

[b] School of Chemistry and Materials Science, University of Science and Technology of China, Hefei 230026, PR China. Wenya Cai and Xianghu Tang contributed equally to this work.

Reference

1. S. C. Tang, S. Vongehr and X. K. Meng, *Journal of Materials Chemistry*, 2010, **20**, 5436-5445.
2. J. Zeng, Q. Zhang, J. Y. Chen and Y. N. Xia, *Nano Letters*, 2010, **10**, 30-35.
3. J. Wang, X. B. Zhang, Z. L. Wang, L. M. Wang, W. Xing and X. Liu, *Nanoscale*, 2012, **4**, 1549-1552.
4. M. H. Rashid, R. R. Bhattacharjee, A. Kotal and T. K. Mandal, *Langmuir*, 2006, **22**, 7141-7143.
5. W. Xie, B. Walkenfort and S. Schlucker, *Journal of the American Chemical Society*, 2013, **135**, 1657-1660.
6. E. Cortes, P. G. Etchegoin, E. C. Le Ru, A. Fainstein, M. E. Vela and R. C. Salvarezza, *Journal of the American Chemical Society*, 2010, **132**, 18034-18037.
7. K. N. Heck, B. G. Janesko, G. E. Scuseria, N. J. Halas and M. S. Wong, *Journal of the American Chemical Society*, 2008, **130**, 16592-16600.
8. V. Joseph, C. Engelbrekt, J. D. Zhang, U. Gernert, J. Ulstrup and J. Kneipp, *Angewandte Chemie-International Edition*, 2012, **51**, 7592-7596.
9. W. Xie, C. Herrmann, K. Kompe, M. Haase and S. Schlucker, *Journal of the American Chemical Society*, 2011, **133**, 19302-19305.
10. Z. Q. Tian, Z. L. Yang, B. Ren, J. F. Li, Y. Zhang, X. F. Lin, J. W. Hu and D. Y. Wu, *Faraday Discussions*, 2006, **132**, 159-170.
11. N. T. Flynn and A. A. Gewirth, *Journal of Raman Spectroscopy*, 2002, **33**, 243-251.
12. S. Guo, S. Dong and E. Wang, *Chemistry-a European Journal*, 2009, **15**, 2416-2424.
13. Z. Y. Bao, J. Y. Dai, D. Y. Lei and Y. C. Wu, *Journal of Applied Physics*, 2013, **114**.
14. H. Deng, X. L. Li, Q. Peng, X. Wang, J. P. Chen and Y. D. Li, *Angewandte Chemie-International Edition*, 2005, **44**, 2782-2785.
15. S. S. R. Dasary, A. K. Singh, D. Senapati, H. T. Yu and P. C. Ray, *Journal of the American Chemical Society*, 2009, **131**, 13806-13812.
16. D. T. Thompson, *Nano Today*, 2007, **2**, 40-43.
17. S. K. Beaumont, G. Kyriakou and R. M. Lambert, *Journal of the American Chemical Society*, 2010, **132**, 12246-12248.
18. J. T. Krug, G. D. Wang, E. Sr and S. M. Nie, *Journal of the American Chemical Society*, 1999, **121**, 9208-9214.
19. M. Schrinner, M. Ballauff, Y. Talmon, Y. Kauffmann, J. Thun, M. Moller and J. Breu, *Science*, 2009, **323**, 617-620.
20. J. Lee, J. C. Park and H. Song, *Advanced Materials*, 2008, **20**, 1523-1528.
21. B. O. Skadtchenko and R. Aroca, *Spectrochimica Acta Part a-Molecular and Biomolecular Spectroscopy*, 2001, **57**, 1009-1016.
22. R. A. Alvarez-Puebla, D. S. Dos Santos and R. F. Aroca, *Analyst*, 2004, **129**, 1251-1256.
23. Q. Q. Ding, H. L. Liu, L. B. Yang and J. H. Liu, *Journal of Materials Chemistry*, 2012, **22**, 19932-19939.
24. X. Zhou, F. Zhou, H. L. Liu, L. B. Yang and J. H. Liu, *Analyst*, 2013, **138**, 5832-5838.